LETTER

A Novel Search Approach for Blur Kernel Estimation of Defocused Image Restoration

Sangwoo AHN[†], *Nonmember and* **Jongwha CHONG**[††a)], *Member*

SUMMARY In this letter, we propose a novel search approach to blur kernel estimation for defocused image restoration. An adaptive binary search on consensus is the main contribution of our research. It is based on binary search and random sample consensus set (RANSAC). Moreover an evaluating function which uses a histogram of gradient distribution is proposed for assessing restored images. Simulations on an image benchmark dataset shows that the proposed algorithm can estimate, on average, the blur kernels 15.14% more accurately than other defocused image restoration algorithms.

key words: *defocused image, out-of-focus, blind image deconvolution, RANSAC, gradient distribution*

1. Introduction

Defocused blurring is the most well-known degrading function that occurs frequently in images. In a camera system, focusing has an important role, because defocusing the lens causes the captured image to lose its sharpness and other features. Much research on defocused image restoration has been conducted in the past few years [1]–[4].

The core algorithm of defocused image restoration is the blur kernel estimation. Selecting a useful and relevant search algorithm is important to improve blur kernel estimation performance. Recent research has proposed search algorithms such as particle swarm optimization (PSO) and genetic algorithm (GA) to cope with blur kernel estimation [3], [4]. Both of these algorithms belong to a priori blur identification method because the parameters of blur model can be estimated by the evolutionary learning. Each particle of these methods represents a probable PSF and is updated according to the evaluating functions which are the wavelet and optical transfer functions (OTF), for the PSO and GA, respectively. These methods generate reliable estimation results for blur kernel estimation but are not without problems of their own. Local optima, terminating criterion and decision problems are well-known weaknesses of these methods. There still remains some room for improvement in the computational cost of a search algorithm and accuracy of its evaluating function. That is to say, search algorithms with reduced complexity but preserved accuracy and improved evaluating functions have long been considered important research topics. The aim of our research is to develop efficient methods for addressing the above issue.

In this letter, a novel search algorithm for blur estimation is proposed and a histogram of gradient (HOG) method is applied for more accurate assessment of restored images than the current state-of-the-art allows.

2. Defocused Image Model

To solve a defocused image restoration problem, mathematical models are required for the natural processes of image generation and formation. The blurring process is most often modeled as follows.

$$o(i, j) = f(i, j) \otimes h(i, j) + n(i, j) \tag{1}$$

where i and j are the coordinates of the images, o is observed image, f is the original image, h is the blur kernel and n is additive white Gaussian noise. In Eq. (1), the blur kernel must be estimated to restore the original image. The blur kernel which is called variously the impulse response function, the blur function or the point spread function can be caused by motion blur, defocus and atmospheric turbulence.

The blur kernel estimation of defocused images is the target of the proposed algorithm. The defocused blur caused by a system with a circular aperture can be modeled as uniform disk [5], [6] like follows.

$$h(i, j) = \begin{cases} \dfrac{1}{\pi R^2}, if \sqrt{i^2 + j^2} \le R \\ 0, if \sqrt{i^2 + j^2} > R \end{cases} \tag{2}$$

where i and j are the image coordinates, h is the defocused kernel and R is the blur radius. This defocused kernel model is simple but it is known to be effective. In Eq. (2), the defocused kernel is determined by finding R. Therefore, the searching for an accurate R of a defocused image is the purpose of our research.

3. Proposed Algorithm

As shown in Fig. 1, the proposed algorithm consists of three parts: PSF estimation, image restoration and image assessment. In the first step, PSF estimation, we estimate a probable PSF with an adaptive binary search on the consensus

Manuscript received May 17, 2012.
Manuscript revised October 24, 2012.
[†]The author is with the Department of Nanoscale Semiconductor Engineering, Hanyang University, 17 Haengdang-Dong, Seongdong-Gu, Seoul, 180–8585, Rep. of Korea.
[††]The author is with the Department of Electronics and Computer Engineering, Hanyang University, 17 Haengdang-Dong, Seongdong-Gu, Seoul, 180–8585 Rep. of Korea.
a) E-mail: jchong@hanyang.ac.kr (Corresponding author)
DOI: 10.1587/transinf.E96.D.754

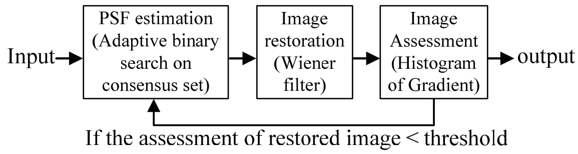

Fig. 1 Block diagram of the proposed algorithm.

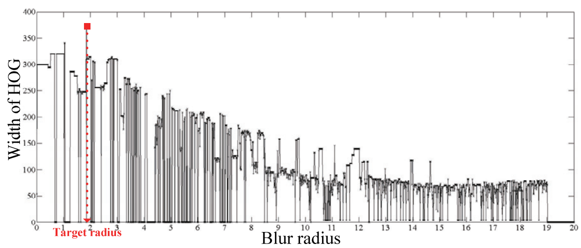

Fig. 2 Example of searching radius.

Algorithm 1: Adaptive binary search on consensus set

Data: R = {0, 0.0001, 0.0002, … , 19.999, 20}
Result: r_{max}
1 Equal sampling interval method ($\text{interval}_1 = 2$)
2 **for** $i = 0$ to 9 **do**
3 **if** $V(r_i)$>threshold **then** (V is evaluating function)
4 Subset $S_i = \{r_i - 1 \le r < r_i + 1\}$ is selected
5 Num_subset = Num_subset+1
6 **else** discard
7 **end**
8 **if** interval == 1 **then go** to 11
9 Equal sampling interval method ($\text{interval}_2 = 1$)
10 **go** to 2
11 Adaptive search on S_i
12 **if** $V(r_{i,left}) > V(r_{i,right})$
13 **then** $S_{i,right}$ is discarded
14 **else**
15 **then** $S_{i,left}$ is discarded
16 size of $S_{i,selected}$ is adjusted by ratio ($V_{prev}/V_{current}$)
17 **if** $N(S_{i,selected}) == 1$ **then**
18 $r_{i,max} = S_{i,selected}$
19 Num_subset = Num_subset – 1
20 **go** to 22
21 **else go** to 11
22 **if** Num_subset == 0 **then**
23 **return** $r_{max} = \max(r_{i,max})$
24 **else go** to 11

* $V(r)$ is the score of the evaluating function at the radius 'r'. $r_{i,left}$ and $r_{i,right}$ are the representative of $S_{i,left}$ and $S_{i,right}$. $S_{i,left}$ and $S_{i,right}$ are derived by dividing subset S_i into two, left side and right side. $N(S)$ means the number of the subset.

Fig. 3 Algorithm of adaptive binary search on consensus set.

set. In the second step, a given image is restored with an estimated PSF. In the third step, a restored image from the previous step is assessed by a HOGbased evaluating function. This iteration scheme is terminated when the assessment result is above the threshold set by experiments.

3.1 Adaptive Binary Search on Consensus Set

Assuming that the evaluating scores of each candidate radius discussed in the next section can be estimated exactly, then the searching radius is a simple problem that finds its maximum value as shown in Fig. 2. However, the number of candidate radii is too numerous to calculate point by point; searching for the target radius by this method requires high cost and a long period of time. Therefore, an adaptive binary search on the consensus set is proposed, which will make the computation cost low and yet still maintain accuracy.

The proposed adaptive binary search on the consensus set is based on two effective algorithms. One is a binary search and the other is a random sample consensus (RANSAC). The procedure of the algorithm is described in Fig. 3. The proposed search algorithm starts with a twostep sampling of equal intervals. The initial subset is called the consensus set for a probable PSF and is determined with the twostep equal sampling interval method in line 1-10. The original binary search is a simple guessing algorithm in which one is given an ordered list and finds the specific value [7]. However, in the proposed algorithm, an adaptive binary search is applied to select subsets with a high possibility of containing the target value, as in lines 11-15.

The original RANSAC algorithm is repeatedly executed as follows [8]. First, subsets of the input data are randomly selected and model parameters fitting these subsets are computed. Then, the quality of the parameters is evaluated on the input data. The process is terminated when the probability of finding a better model becomes lower than a userdefined threshold. Two characteristics of RANSAC are applied to the binary search algorithm. One is the subset based search described in line 1-10; the other is the adjustment of the set size based on evaluating scores described in lines 11-16. The adaptive binary search on consensus set is terminated when the number of items in the consensus set is one, as in lines 17-24.

The adaptive binary search is thus advantageous because the number of iterations for a search is reduced by using the consensus set instead of the entire candidate set and the problem with local optima is avoided by adjusting the set size of the method.

3.2 Histogram of Gradient Distribution

We are able to restore defocused images by numerous iterations when the evaluating function is accurate. Because it is the evaluating function that determines whether a restored image is focused or not. In other words, the accuracy of the evaluating function has a significant influence on the accuracy of the proposed algorithm.

The characteristics of HOG are used to evaluate the degree of blur of a single image. Recent research shows that a HOG can represent the degree of blur; one of the basic characteristics of a HOG is that clear images tend to have large gradient values while blurred images have small ones. This is because each point of a blurred image is spread to the neighboring points by blurring and this spreading is what makes the gradient small. Calculating a histogram for an image is often very time consuming; nevertheless, ensuring the accuracy of the evaluating function is important enough to warrant its use. The HOG used for evaluating is written as follows.

$$\begin{aligned} H &= \log(\textstyle\sum (G_x[g] + G_y[g])) \\ G_x &= I \otimes s_x, G_y = I \otimes s_y \end{aligned} \tag{3}$$

where H is the HOG, I is the input image, g is the gradient value, G_x and G_y are the x- the y-direction gradient image, respectively, and s_x and s_y are the x and y direction filter kernels set to [1,-1] and $[1,-1]^{\mathrm{T}}$, respectively. The range of $\sum$ is from -255 to 255.

The notation of the HOG is described by Fig. 4. It shows a focused image, a defocused image and the histogram of their gradient magnitudes. The distribution shows that HOG can distinguish between the focused and defocused images. However, there is the issue of how to measure the width of these histograms. Other researchers use heavy-tailed distributions to approximate parameters but we simply have to estimate the width of the histogram distribution. Therefore, in the proposed algorithm, the width is driven by two points with the same y-value a simple method that repeatedly draws a line parallel to the x-axis and checks which points are matched. This can be described by Eq. (4)

$$Q = \min_{w}\{w|H(w) - H(-w) = 0\} \tag{4}$$

where H is the HOG which is calculated by Eq. (3) and w which is used for measuring width.

3.3 Image Reconstruction

Defocused images are modeled by convolution of the original image and blur kernel. Then, defocused images are restored by the deconvolution algorithm. The most famous deconvolution algorithm, the Wiener filter is used in the restoring algorithm in this paper. The wiener filter equation in the frequency domain is as follows.

$$\hat{F}(u,v) = \left[\frac{1}{H(u,v)}\frac{|H(u,v)|^2}{|H(u,v)|^2 + K}\right] O(u,v) \tag{5}$$

where $\hat{F}$ is the restored image, H is the blur kernel, O is observed image and K is a constant value to adjust noise effect.

4. Simulation

Simulations are performed on the Cameraman, Lena and Tampere Image Database 2008 (TID 2008) [9]. The images all have the same resolution of 512×512 pixels.

In order to evaluate the accuracy of the proposed algorithm, two simulations were performed. The first was a simulation for subjective evaluation of the image, comparing the resulting images against those of [2] and [4]. The second was a simulation for objective evaluation and compared the estimated R against those of [3], [4] and [10], which all use the same mathematical method to model the defocused images. The parameters of [4] were: population number = 30 and iterative number = 20. The parameters of [3] were: particle number = 30, $c_1 = 1.193$, $c_2 = 1.193$, $w = 0.79$ and $maxG = 20$ given in each paper. Simulation of [2] was performed with the software released on their website.

Figure 5 shows that the proposed algorithm can restore a defocused image to a greater sharpness than other algorithms. Figure 5 (b), which was restored with the proposed algorithm, has sharp edge lines but some color distortion Future work remains in solving the color distortion problem by studying the restoration filter. Figure 5 (c) still retains some blur and noise because of low accuracy estimation of R. Figure 5 (d) looks sharp, but shows some artifacts near the lines.

A second simulation is performed on algorithms that

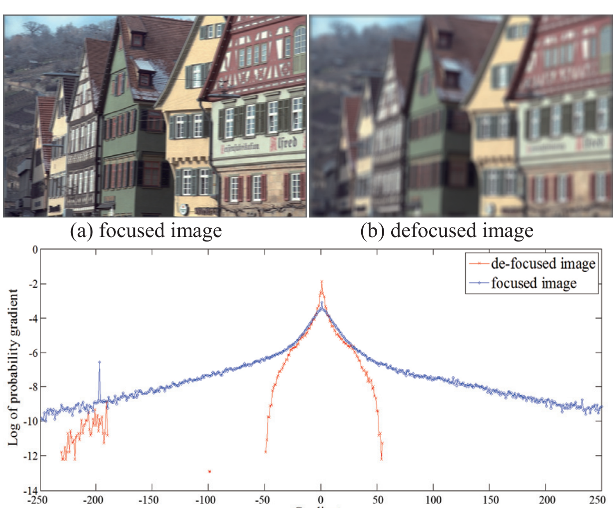

(a) focused image (b) defocused image

(c) Histogram of gradient distribution

Fig. 4 Comparing HOG between focused and defocused images.

(a) defocused image (b) result image of proposed

(c) result image of [4] (d) result image of [2]

Fig. 5 Comparing result images.

Table 1 Estimated R of cameraman.

Real R	Method			
	[3]	[4]	[10]	Proposed
3	2.8465	2.2648	4.9753	2.8760
5	5.0408	5.0398	4.7122	5.0317
7	7.1098	7.1310	4.5870	6.9825
9	9.1690	9.1718	6.4839	9.087

Table 2 Estimated R of Lena.

Real R	Method			
	[3]	[4]	[10]	Proposed
3	2.7546	2.4980	3.1771	2.8846
5	4.6764	5.0583	5.2089	5.1072
7	7.1018	7.1007	7.3120	7.0873
9	9.1031	9.0998	9.5371	8.9324

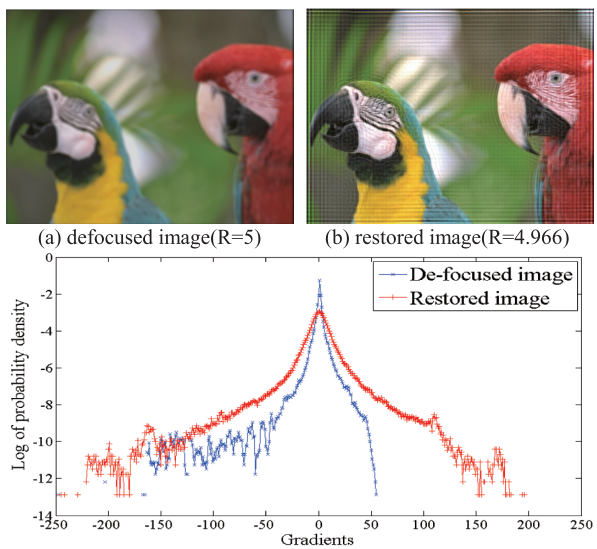

(a) defocused image(R=5) (b) restored image(R=4.966)

(c) the HOG of (a) and (b)

Fig. 6 Simulation results performed on Birds image of [9]. This shows that the restored image has wider width on the HOG.

use the same mathematical model of the defocused images. The accuracy of each algorithm can be evaluated by its radius values. Table 1 and Table 2 show that the proposed algorithm is more accurate than the others because that the evaluating function in the proposed algorithm is more accurate than those in the other algorithms.

Figure 6 show pairs of defocused images and restored images to illustrate the utility of the proposed algorithm further. Figure 6 shows that the proposed algorithm can be used for significantly defocused images.

5. Conclusion

In this paper, we propose two algorithms for the restoration of defocused images. One algorithm is an adaptive binary search on the consensus set and the other is an evaluating function that uses the HOG. The proposed algorithm has greater accuracy than the other algorithms. Adaptive binary search helps the proposed algorithm avoid the local-maximum problem and also increases the accuracy of the proposed algorithm.

Acknowledgments

This research was supported by Hynix Semiconductor Inc., and the MKE (The Ministry of Knowledge Economy), Korea, under the ITRC (Information Technology Research Center) support program supervised by the NIPA (National IT Industry Promotion Agency)" (NIPA-2012-H0301-12-1011). The IDEC provide research facilities for this study. This work was supported by the Brain Korea 21 Project in 2012.

References

[1] L. Yuan, J. Sun, L. Quan, and H.-Y. Shum, "Image deblurring with blurred/noisy image pairs," ACM Trans. Graphics, vol.26, no.1, article.1, 2007.

[2] R. Fergus, B. Singh, A. Hertzmann, S.T. Roweis, and W.T. Freeman, "Removing camera shake from a single photograph," ACM Trans. Graphics, vol.25, no.3, pp.787–794, 2006.

[3] M.E Moghaddam, "Out of focus blur estimation using genetic algorithm," International Conference on Systems, Signals and Image Processing, pp.417–420, June 2008.

[4] T.Y. Sun, S.J. Ciou, C.C. Liu, and C.L. Huo, "Out-of-focus blur estimation for blind image deconvolution: Using particle swarm optimization," IEEE International Conference on Systems, Man and Cybernetics, pp.1627–1632, Oct. 2009.

[5] S. Wu, W. Lin, L. Jian, W. Xiong, and L. Chen, "An objective out-of-focus blur measurement," International Conference on Information, Communications and Signal Processing, pp.334–338, 2005.

[6] R.L. Lagendijk and J. Biemond, "Basic methods for image restoration and identification," in Hand Book of Image and Vedio Processing, chapter B, pp.125–140, Academic Press, 2000.

[7] R. Nowak, "Generalized binary search," Annual Allerton Conference on Communication, Control and Computing, pp.568–574, Sept. 2008.

[8] O. Chum and J. Matas, "Optimal randomized RANSAC," IEEE Trans. Pattern Anal. Mach. Intell., vol.30, no.8, pp.1472–1482, Aug. 2008.

[9] N. Ponomarenko, V. Lukin, A. Zelensky, K. Egiazarian, M. Carli, and F. Battisti, "TID2008 - A database for evaluation of full-reference visual quality assessment metrics," Advances of Modern Radioelectronics, vol.10, pp.30–45, 2009.

[10] T.Y. Sun, C.C. Liu, Y.P. Jheng, J.H. Jheng, S.J. Tsai, and S.T. Hsieh, "Blind image deconvolution via particle swarm optimization with entropy evaluation," International Conference on Intelligent Systems Design and Applications, vol.2, pp.256–270, 2008.